Redox Biology 14 (2018) 20–34

Contents lists available at ScienceDirect

Redox Biology

journal homepage: www.elsevier.com/locate/redox

Reduced levels of methyltransferase DNMT2 sensitize human fibroblasts to oxidative stress and DNA damage that is accompanied by changes in proliferation-related miRNA expression

Anna Lewinska[a,*], Jagoda Adamczyk-Grochala[a], Ewa Kwasniewicz[a], Anna Deregowska[b,c], Ewelina Semik[d], Tomasz Zabek[d], Maciej Wnuk[c]

[a] Laboratory of Cell Biology, University of Rzeszow, Pigonia 1, 35-310 Rzeszow, Poland
[b] Postgraduate School of Molecular Medicine, Medical University of Warsaw, Warsaw, Poland
[c] Department of Genetics, University of Rzeszow, Rzeszow, Poland
[d] Laboratory of Genomics, National Research Institute of Animal Production, Balice n. Cracow, Poland

ARTICLE INFO

Keywords:
DNMT2
Fibroblasts
Oxidative stress
Genotoxicity
Proliferation
miRNAs

ABSTRACT

Methyltransferase DNMT2 is suggested to be involved in the regulation of numerous processes, however its biological significance and underlying molecular mechanisms remain elusive. In the present study, we have used WI-38 and BJ human fibroblasts as an in vitro model system to investigate the effects of siRNA-based DNMT2 silencing. DNMT2-depleted cells were found to be sensitive to oxidative stress conditions as judged by increased production of reactive oxygen species and susceptible to DNA damage that resulted in the inhibition of cell proliferation. DNMT2 silencing promoted upregulation of proliferation-related and tumor suppressor miRNAs, namely miR-28-3p, miR-34a-3p, miR-30b-5p, miR-29b-3p, miR-200c-3p, miR-28-5p, miR-379-5p, miR-382-5p, miR-194-5p, miR-193b-3p and miR-409-3p. Moreover, DNMT2 silencing induced cellular senescence and DNMT2 levels were elevated in replicatively senescent cells. Taken together, we found that DNMT2 may take part in the regulation of cell proliferation and longevity in human fibroblasts and speculate that the manipulation of DNMT2 levels that limits cell proliferation may be potentially useful anticancer strategy.

1. Introduction

Human DNA methyltransferase 2 (DNMT2), a member of nucleic acid modification enzyme family, catalyzes the transfer of a methyl group from the cofactor *S*-adenosyl-methionine (SAM) to the carbon-5 of cytosine residues [1,2]. DNMT2 is suggested to be both DNA and RNA methyltransferase (MTase) [1,2], but more recently DNMT2-based DNA methylation has been shown to be marginal [3,4] and DNMT2 has been reported to be a highly specific $tRNA^{Asp}$ methyltransferase [4]. Despite numerous studies involving different model systems, the biological role of DNMT2 is still enigmatic [1,2,4–13].

More recently, human DNMT2 has been reported to participate in RNA processing during cellular stress [14]. Moreover, we have found that the levels of human DNMT2 and mouse Dnmt2 are elevated during oxidative stress conditions being a part of an adaptive response to protect RNA from degradation [15–17]. This phenomenon seems universal as oxidant-mediated upregulation of human DNMT2 and mouse Dnmt2 was observed in normal cells, immortalized cells and cancer cells [15–17] and sustained even after 6 days of removal of oxidative stress-promoting agents [17]. Overexpression of DNMT2 homologs also conferred resistance to oxidative and nitrosative stresses in lower organisms [18–20].

As dDnmt2 is a pro-longevity factor in the fruit fly *Drosophila melanogaster* [18] and there are no data on DNMT2-mediated effects on human cell vitality, viability and reproductive potential, in the present study, we have used siRNA-based system to diminish DNMT2 levels in two human fibroblast cell lines, namely WI-38 and BJ cells and found that reduced levels of DNMT2 limited cell proliferation and induced cellular senescence that was mediated by oxidative stress, DNA damage and changes in proliferation-related miRNAs. The effects of hydrogen peroxide-induced oxidative stress were also addressed. DNMT2 levels were shown to be upregulated in replicatively senescent cells that suggest that DNMT2 may be considered as a novel regulator of longevity in human fibroblasts.

* Corresponding author.
E-mail address: lewinska@ur.edu.pl (A. Lewinska).

http://dx.doi.org/10.1016/j.redox.2017.08.012
Received 24 July 2017; Received in revised form 11 August 2017; Accepted 18 August 2017
Available online 18 August 2017

2. Materials and methods

2.1. Cell culture

Human fetal lung fibroblasts WI-38 (ATCC® CCL-75™) and human foreskin fibroblasts BJ (ATCC® CRL-2522™) were obtained from American Type Culture Collection (ATCC, Manassas, Virginia, USA). According to ATCC certificate, WI-38 cells (maximum PDL = 50 ± 10) were provided at population doubling level (PDL) 31.2 and BJ cells (maximum PDL = 72) at PDL 24. Fibroblasts (10,000 cells/cm^2) were cultured at 37 °C in Dulbecco's Modified Eagle's medium (DMEM) containing 10% fetal calf serum (FCS), 100 U/ml penicillin, 0.1 mg/ml streptomycin and 0.25 μg/ml amphotericin B (Sigma-Aldrich, Poznan, Poland) in a cell culture incubator in the presence of 5% CO_2. Fibroblasts were passaged using trypsin-EDTA solution (Sigma-Aldrich) and PDL was calculated according to the formula: PDL = PDL_i + 3.322 (log at_h – log at_s); where PDL_i is an initial population doubling level, at_h is a total number of cells at harvest and at_s is a total number of cells at seed. Except of replicative senescence experiments, proliferatively active fibroblasts were used, namely WI-38 cells at PDLs from 34 to 43 and BJ cells at PDLs from 27 to 43.

2.2. siRNA transfection

For RNAi-based transient silencing of *DNMT2* mRNA, cells were transfected with DNMT2 siRNA (h) (Santa Cruz Biotechnology, Dallas, Texas, USA, sc-35205) using Lipofectamine® RNAiMAX Reagent (Thermo Fisher Scientific, Waltham, Massachusetts, USA) according to the manufacturer's instructions. As a control, cells were transfected with control siRNA (fluorescein conjugate)-A (Santa Cruz Biotechnology, sc-36869). Silencing of DNMT2 was monitored using qRT-PCR and probes 21 (left primer ttggcattccaaattcaagg, right primer ggggaactccatcagtacca) and 65 (left primer tcctaaagaaatagcaaatctccttg, right primer cgctgtttcactgttatcttctca) from Universal Probe Library (Roche, Basel, Switzerland, 04686942001 and 04688643001, respectively), and Western blotting and anti-DNMT2 anti-bodies (Santa Cruz Biotechnology and Thermo Fisher Scientific and Abcam, Cambridge, UK). Briefly, RNA was isolated using GenElute™ Mammalian Total RNA Miniprep Kit (Sigma-Aldrich) and cDNA was synthesized using 2 μg of RNA and Transcriptor First Strand cDNA Synthesis Kit (Roche). LightCycler® 480 Real-Time PCR System and LightCycler® 480 Probes Master were used (Roche) according to the manufacturer's instructions. *G6PD* glucose-6-phosphate dehydrogenase gene was used as a housekeeping gene. Results are expressed as the target/reference ratio of each sample divided by the target/reference ratio of a calibrator. Western blotting protocol can be found within the subsection Western blotting.

2.3. Apoptosis

Fibroblasts were treated with 100 μM hydrogen peroxide (HP) (Sigma-Aldrich) for 2 h and then cultured for 1, 2 or 7 days. HP concentration and exposure time were selected on the basis of MTT results (data not shown). HP-induced apoptosis was evaluated using Muse™ Cell Analyzer and Muse™ Annexin V and Dead Cell Assay Kit (Merck Millipore, Warsaw, Poland) as described elsewhere [21].

2.4. Cell cycle analysis

Fibroblasts were treated with 100 μM HP for 2 h and DNA-based cell cycle analysis was performed using Muse™ Cell Analyzer and Muse™ Cell Cycle Kit according to the manufacturer's instructions (Merck Millipore) [22].

2.5. Senescence-associated β-galactosidase activity (SA-β-gal)

Fibroblasts were treated with 100 μM HP for 2 h, and 7 days after HP removal SA-β-gal activity was analyzed as described elsewhere [22].

2.6. Oxidative stress

Fibroblasts were treated with 100 μM HP for 2 h and reactive oxygen species (ROS), total and mitochondrial superoxide production were evaluated using a chloromethyl derivative of H_2DCF-DA (CM-H_2DCF-DA), dihydroethidium and MitoSOX™ Red reagent, respectively (Thermo Fisher Scientific) [23]. Protein carbonylation was assayed using an OxyBlot™ Protein Oxidation Detection Kit (Merck Millipore) using the standard protocol according to the manufacturer's instructions [23].

2.7. Genotoxicity and DNA damage response

Neutral comet assay (analysis of DNA double-strand breaks, DSBs) was performed upon stimulation with 100 μM HP for 2 h as described comprehensively elsewhere [24]. Comets (n = 200) were analyzed using OpenComet, an open-source software tool (http://www.cometbio.org/) [25]. The Olive Tail Moment (OTM) was used for the assessment of DNA integrity [26]. Micronuclei production was revealed using a BD™ Gentest Micronucleus Assay Kit according to the manufacturer's instructions (Becton Dickinson, Franklin Lakes, New Jersey, USA). The phosphorylation status of ATM and H2AX was evaluated using Muse™ Cell Analyzer and Muse™ Multi-Color DNA Damage kit (Merck Millipore) as described elsewhere [22].

2.8. Immunostaining

An immunostaining procedure was used as described comprehensively elsewhere [21]. The following primary and secondary antibodies were used: anti-Ki67 (1:500, PA5-19462), anti-53BP1 (1:100, PA5-17578) (Thermo Fisher Scientific) and anti-DNMT2 (1:200, sc-365001, ab82659, PA5-11187) and a secondary antibody conjugated to Texas Red (1:1000, T2767) (Thermo Fisher Scientific). Digital cell images were captured using imaging cytometry (In Cell Analyzer 2000 equipped with a high performance CCD camera, GE Healthcare, Little Chalfont, UK). Ki67 signals were scored [%], 53BP1 foci were scored per nucleus and DNMT2 cytosolic signals were presented as relative fluorescence units (RFU). Moreover, DNMT2 nuclear/cytosolic ratio was calculated.

2.9. qRT-PCR using TaqMan® arrays

Fibroblasts were treated with 100 μM HP for 2 h and RNA was extracted using GenElute™ Mammalian Total RNA Miniprep Kit (Sigma-Aldrich) and cDNA was synthesized using 2 μg of RNA and Transcriptor First Strand cDNA Synthesis Kit (Roche) according to the manufacturer's instructions. The expression patterns of selected genes, namely cyclins, cell cycle regulation-associated genes, DNA methylation and transcriptional repression-associated genes were investigated using Applied Biosystems StepOnePlus™ Real-Time PCR System and dedicated Real-Time PCR TaqMan® Array Plates, namely TaqMan® Array 96-Well FAST Plate Human Cyclins and Cell Cycle Regulation (4418768, Applied Biosystems™) and TaqMan® Array 96-Well FAST Plate Human DNA Methylation and Transcriptional Repression (4418772, Applied Biosystems™), respectively, according to the manufacturer's instructions. *GUSB* gene was used as a reference gene. Heat maps were created using Genesis 1.7.7 software [27] (https://genome.tugraz.at/genesisclient/genesisclient_download.shtml) based on ΔCt values and selected functions, namely log2 transform ratio and hierarchical clustering functions.

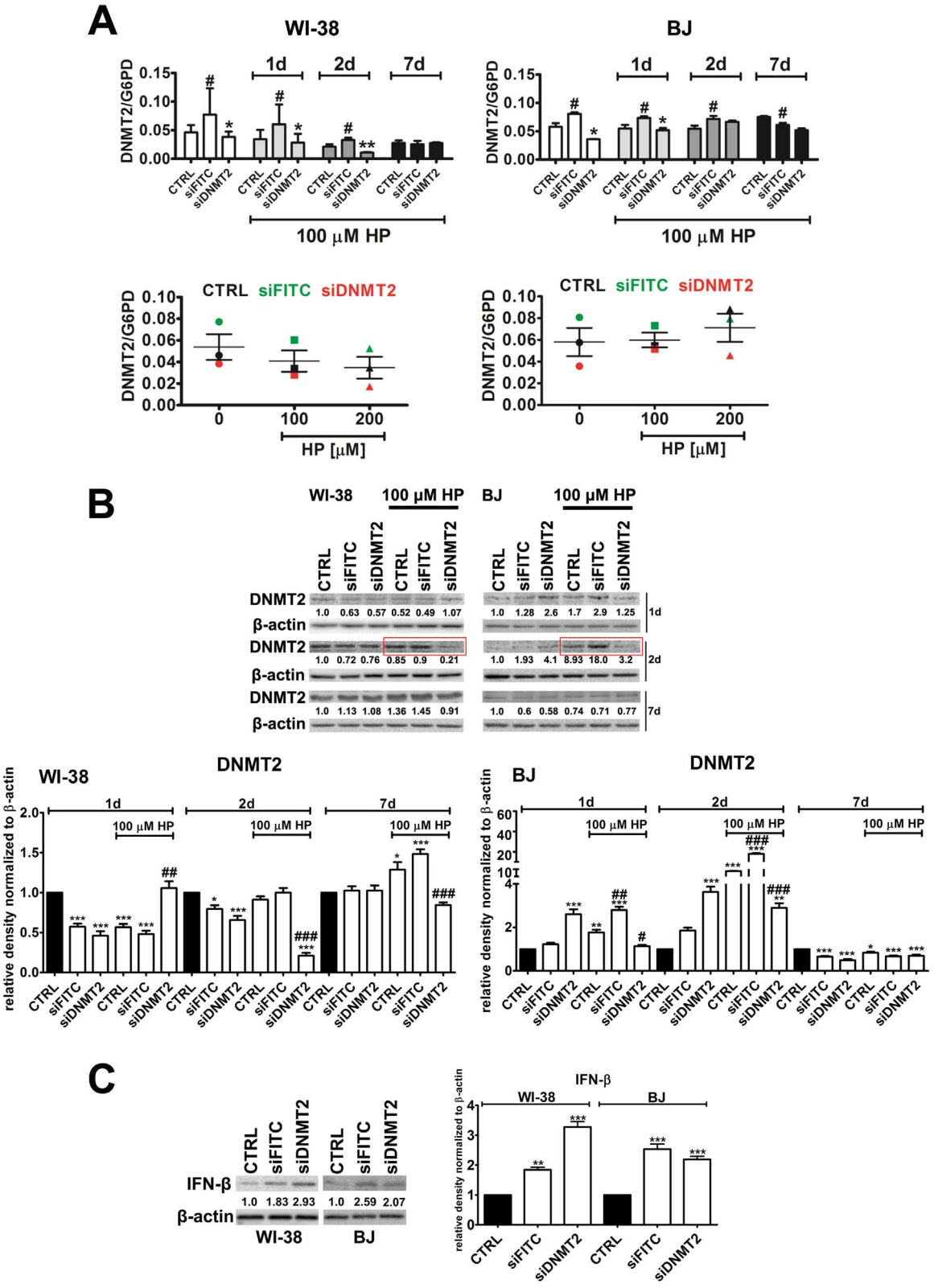

Fig. 1. DNMT2 silencing and siRNA-mediated immunogenic response in WI-38 and BJ human fibroblasts. (A) The analysis of DNMT2 mRNA levels using qRT-PCR. DNMT2/G6PDH ratio is presented. The effect of HP treatment is also included. Fibroblasts were treated with 100 μM HP for 2 h and 1, 2 and 7 days after HP removal DNMT2 mRNA levels were assayed (upper panel, bars indicate SEM, n = 3, $^{\#}p < 0.05$ compared to CTRL, $^{*}p < 0.05$, $^{**}p < 0.01$ compared to control siRNA (siFITC) (ANOVA and Dunnett's *a posteriori* test) or fibroblasts were treated with 100 μM or 200 μM HP for 2 h and 24 h after HP removal DNMT2 mRNA levels were assayed (lower panel, scatter plots, bars indicate SEM). (B) The analysis of DNMT2 protein levels using Western blotting. HP effect on DNMT2 silencing is highlighted (red frames). Data were normalized to β-actin. Bars indicate SD, n = 3, $^{*}p < 0.05$, $^{**}p < 0.01$, $^{***}p < 0.001$ compared to CTRL, $^{\#}p < 0.05$, $^{\#\#}p < 0.01$, $^{\#\#\#}p < 0.001$ compared to HP-treated CTRL (ANOVA and Dunnett's *a posteriori* test). (C) The analysis of IFN-β levels using Western blotting. Data were normalized to β-actin. Bars indicate SD, n = 3, $^{**}p < 0.01$, $^{***}p < 0.001$ compared to CTRL (ANOVA and Dunnett's *a posteriori* test). Proliferatively active fibroblasts were used, namely WI-38 cells at PDLs from 34 to 43 and BJ cells at PDLs from 27 to 43. CTRL, non-transfected control fibroblasts; siFITC, fibroblasts transfected with control FITC-conjugated siRNA; siDNMT2, fibroblasts transfected with DNMT2 siRNA. (For interpretation of the references to color in this figure legend, the reader is referred to the web version of this article.)

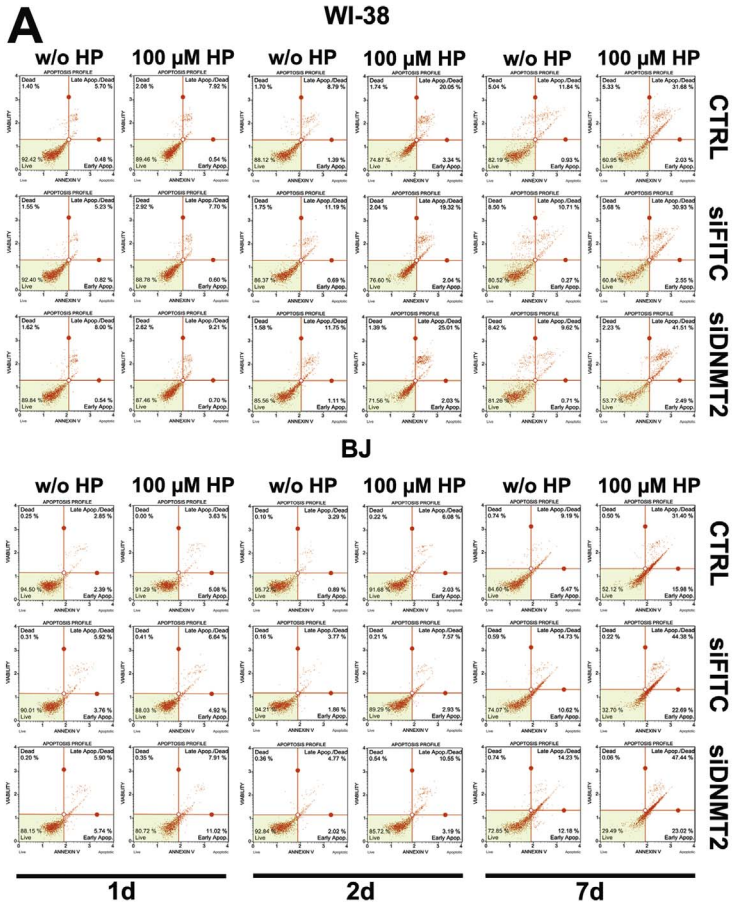

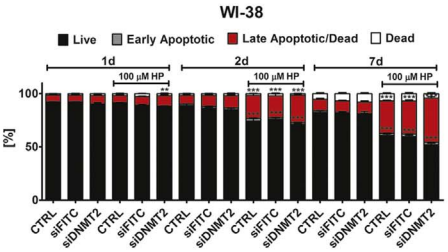

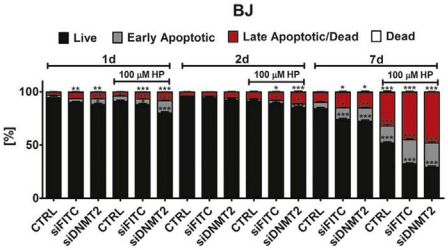

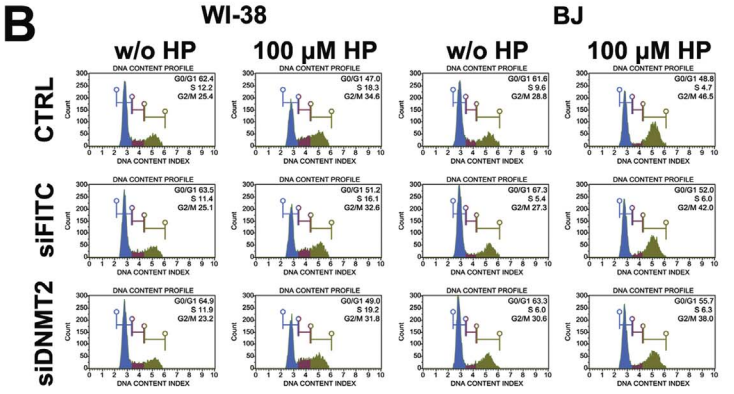

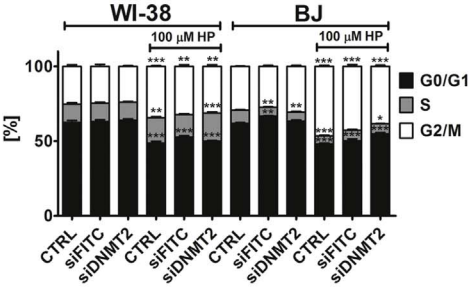

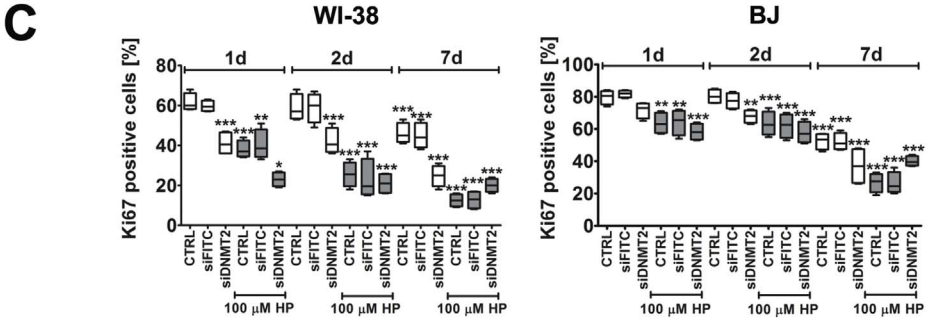

(caption on next page)

Fig. 2. DNMT2 silencing-mediated effects on apoptosis (A), cell cycle (B) and cell proliferation (C). HP treatment is also considered. (A) DNMT2 silencing enhances HP-induced apoptosis in WI-38 and BJ human fibroblasts. Phosphatidylserine externalization was evaluated using Annexin V staining and flow cytometry. Bars indicate SD, n = 3, $^{*}p < 0.05$, $^{**}p < 0.01$, $^{***}p < 0.001$ compared to CTRL (ANOVA and Dunnett's *a posteriori* test). (B) DNA content-based analysis of cell cycle was performed using flow cytometry. Cells were treated with 100 μM HP for 2 h and then cultured for 24 h. Bars indicate SD, n = 3, $^{*}p < 0.05$, $^{**}p < 0.01$, $^{***}p < 0.001$ compared to CTRL (ANOVA and Dunnett's *a posteriori* test). (C) Cell proliferation was measured using Ki67 immunostaining and imaging cytometry. Ki67 signals were scored [%]. Box and whisker plots are shown, n = 3, $^{*}p < 0.05$, $^{**}p < 0.01$, $^{***}p < 0.001$ compared to CTRL (ANOVA and Dunnett's *a posteriori* test). Proliferatively active fibroblasts were used, namely WI-38 cells at PDLs from 34 to 43 and BJ cells at PDLs from 27 to 43. CTRL, non-transfected control fibroblasts; siFITC, fibroblasts transfected with control FITC-conjugated siRNA; siDNMT2, fibroblasts transfected with DNMT2 siRNA.

2.10. Western blotting

Western blotting protocol was used as described comprehensively elsewhere [28]. The following primary and secondary antibodies were used: anti-p16 (1:200, MA5-17093), anti-p21 (1:500, MA5-14949), anti-p53 (1:500, MA5-12557), anti-DNMT1 (1:500, sc-271729), anti-DNMT2 (1:200 or 1:500, sc-365001, ab82659, PA5-11187), anti-DNMT3A (1:250, sc-373905), anti-DNMT3B (1:500, sc-376043), anti-IFN-β (1:1000, ab176343) or anti-β-actin (1:40000, A3854) (Thermo Fisher Scientific, Santa Cruz, Sigma-Aldrich and Abcam) and secondary antibodies conjugated to HRP (1:50000, A2554, A0545, Sigma-Aldrich). Protein levels were normalized to β-actin.

2.11. DNA and RNA methylation

To measure the levels of 5-methyldeoxycytosine (5-mdC) in DNA, 5-methylcytosine (5-mC) in RNA and N^6-methyladenosine (m^6A) in RNA, ELISA-based assays were used, namely, MethylFlash Methylated DNA 5-mdC Quantification Kit, MethylFlash 5-mC RNA Methylation ELISA Easy Kit and EpiQuik m^6A RNA Methylation Quantification Kit, respectively (EpiGentek, Farmingdale, New York, USA).

2.12. Site-specific methylation of 18S rRNA gene promoter

Promoter sequence of 18S rRNA was obtained from Ghoshal et al. [29]. DNA was isolated using Wizard Genomic DNA Purification Kit (Promega, Germany) and modified with sodium bisulfite using Epitec Bisulfite Conversion Kit (Qiagen, Germany). Investigated regions were amplified using BSPCR primers designed using Methyl Primer Express® Software v1.0 (Supplementary Table 1). BSPCR reaction mixture contained: 10 ng template, 1 × PCR buffer (Tris-HCl, KCl, $(NH_4)_2SO_4$, pH 8.7), 2 mM $MgCl_2$, 0.2 mM dNTP (Applied Biosystems, CA, USA), 0.125 μM starters, 1 U HotStart Taq polymerase (5 U/μl) (Qiagen, Germany) and milliQ water to a final volume of 20 μl. The following BSPCR reaction conditions were: initial denaturation at 95 °C for 15 min, 5 cycles of denaturation at 97 °C for 5 s, annealing for 2 min (2nd T_a in Supplementary Table 1), elongation at 72 °C for 45 s, 35 cycles of denaturation at 97 °C for 5 s, annealing (1st T_a in Supplementary Table 1) for 2 min, elongation at 72 °C for 45 s and final elongation at 72 °C for 7 min. The BSPCR products were digested using enzyme solution mix (1 U/μl SAP and 20 U/μl ExoI) and incubated at 37 °C for 30 min followed by heat inactivation at 80 °C for 15 min. BSPCR products were sequenced from both complementary strands with the use of BigDye® Terminator v3.1 Cycle Sequencing Kit. Sequencing products were purified using BigDye® XTerminator Purification Kit according to manufacturer's instructions and separated in the presence of polymer POP-7 using Genetic Analyzer ABI3130xl (Applied Biosystems, CA, USA). Converted DNA samples showing fuzzy methylated CpG sites in the rRNA gene promoter were amplified in the 50 μl of BSPCR reaction mixture using above-mentioned reaction conditions. BSPCR products were purified using MinElute PCR purification kit (Qiagen, Germany) and cloned into TOPO TA Cloning vector (Thermo Fisher Scientific). 17–23 clones were sequenced using universal primers using BigDye® Terminator v3.1 Cycle Sequencing Kit (Thermo Fisher Scientific). Bisulfite sequencing reads were used for the assessment of the methylation levels in CG context (number of clones with cytosine at particular CpG sites after bisulfite sequence alignment to the unconverted genomic reference) using BISMA software [30].

2.13. miRNA expression profiles

RNA was isolated using GenElute™ Mammalian Total RNA Miniprep Kit (Sigma-Aldrich) and cDNA was synthesized using 100 ng of RNA and EPIK miRNA Panel Assays (Bioline Ltd.) that involved RT Primer Pool, EPIK RT Enzyme, EPIK RT Buffer and RNA Spike according to the supplier's instructions. The expression of 176 miRNAs (http://www.bioline.com/list-of-stemcell-panel-plates#table1) involved in the regulation of cell proliferation, differentiation and stress responses was evaluated using Applied Biosystems StepOnePlus™ Real-Time PCR System and dedicated EPIK Stem Cell miRNA Panel (Hi-ROX Plate 0.1Y, BIO-66035, Bioline Ltd.) according to the manufacturer's instructions. The qRT-PCR products that were amplified after 32 cycles were discarded. The expression profiles were created using Genesis 1.7.7 software (https://genome.tugraz.at/genesisclient/genesisclient_download.shtml) on the basis of global normalized Ct values and log10 to log2, log2 transform ratio and hierarchical clustering functions.

2.14. Statistical analysis

The results represent the mean ± SD from at least three independent experiments. Alternatively, box and whisker plots with median, lowest and highest values or scatter plots with mean and SEM were used. Statistical significance was assessed by 1-way ANOVA using GraphPad Prism 5, and with the Dunnett's multiple comparison test. The differences in miRNA expression between control siRNA- vs DNMT2 siRNA-treated samples were analyzed using Student's *t*-test.

3. Results

3.1. siRNA transfection induces DNMT2-mediated immunogenic response

DNMT2 was silenced at mRNA levels using dedicated siRNA (Fig. 1A).

The silencing effect was augmented upon hydrogen peroxide (HP) treatment (oxidative stress conditions) in WI-38 cells (Fig. 1A). DNMT2 was also downregulated at protein levels in WI-38 cells and the silencing effect was lost after 7 days of cell culture (Fig. 1B). However, reduced levels of DNMT2 protein was also observed after control siRNA transfection (Fig. 1B). HP treatment enhanced silencing effect in DNMT2 siRNA-transfected WI-38 cells compared to HP-treated non-transfected and control siRNA-transfected WI-38 cells, especially after 48 h of HP removal (Fig. 1B, in a red frame). In contrast, silencing effect was observed only after prolonged culture in BJ cells (Fig. 1B). DNMT2 was more downregulated upon HP treatment in DNMT2 siRNA-transfected BJ cells compared to HP-treated non-transfected and control siRNA-transfected BJ cells (Fig. 1B, in a red frame). Thus, DNMT2 protein levels were downregulated in DNMT2 siRNA-transfected fibroblasts only upon oxidative stress conditions and after 48 h of HP removal. Perhaps, the remaining pool of DNMT2 protein is more efficiently degraded in stress conditions compared to control conditions. Surprisingly, *DNMT2* mRNA levels were elevated after transfection with control siRNA that suggest that DNMT2 may be involved in antiviral response (Fig. 1A). Immunomodulatory response upon siRNA transfection was the most accented in DNMT2-silenced WI-38 cells as judged by elevated levels of beta-interferon (IFN-β) (Fig. 1C).

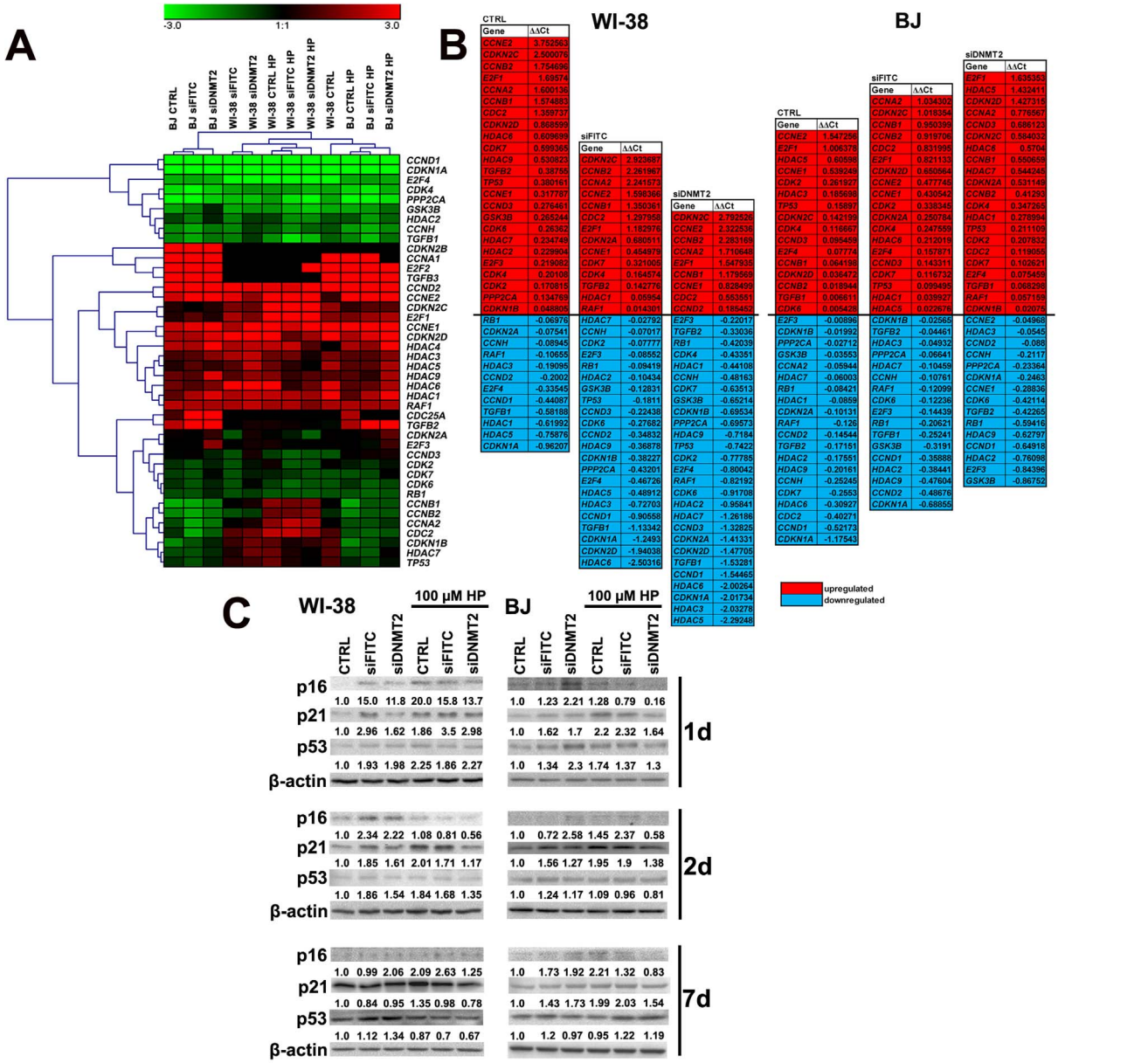

(caption on next page)

Fig. 3. DNMT2 silencing-mediated effects on mRNA (A, B) and protein levels (C, D) of cell cycle regulators. HP treatment is also considered. (A, B) The expression of selected genes involved in the regulation of cell cycle. Cells were treated with 100 μM HP for 2 h and then cultured for 24 h. (A) A heat map generated from qRT-PCR data is shown. Hierarchical clustering was created using Genesis 1.7.7 software. (B) HP-mediated up- (red) and downregulation (blue) of cell cycle genes. ΔΔCt values are shown. (C, D) Western blot analysis of the levels of p16, p21 and p53. Data were normalized to β-actin. Bars indicate SD, n = 3, $^{*}p < 0.05$, $^{**}p < 0.01$, $^{***}p < 0.001$ compared to CTRL (ANOVA and Dunnett's *a posteriori* test). Proliferatively active fibroblasts were used, namely WI-38 cells at PDLs from 34 to 43 and BJ cells at PDLs from 27 to 43. CTRL, non-transfected control fibroblasts; siFITC, fibroblasts transfected with control FITC-conjugated siRNA; siDNMT2, fibroblasts transfected with DNMT2 siRNA. (For interpretation of the references to color in this figure legend, the reader is referred to the web version of this article.)

3.2. DNMT2 silencing sensitizes cells to HP-induced apoptosis

DNMT2 silencing resulted in an increase in apoptotic cell death in the control conditions, especially after 7 days of culture (Fig. 2A).

DNMT2-silenced cells were more sensitive to HP-induced apoptosis than control non-transfected and control siRNA-transfected cells that was observed after 24 h of HP removal in BJ cells and after 48 h of HP removal in WI-38 cells (Fig. 2A). Moreover, 7 days after HP removal, DNMT2-silenced BJ cells were more prone to apoptosis than DNMT2-silenced WI-38 cells (Fig. 2A).

3.3. DNMT2 silencing results in permanent inhibition of cell proliferation

DNMT2 silencing did not promote massive changes in the cell cycle both in the control and stress conditions (HP treatment) compared to unmodified control and control siRNA treatment (Fig. 2B). HP induced G2/M cell cycle arrest, but the level of cells in the G2/M phase of the cell cycle was comparable in DNMT2-silenced cells and control cells (Fig. 2B). In contrast, DNMT2 silencing promoted the inhibition of cell proliferation in the control conditions and of course the cytostatic effect was augmented after HP treatment (Fig. 2C). We have then considered the expression profiles of selected genes involved in the regulation of cell cycle (n = 44) (Fig. 3A and B).

In general, HP treatment stimulated similar changes in gene expression patterns as all HP-treated cell categories were grouped together (Fig. 3A). HP treatment resulted in upregulation of *CDKN2C* (p18), *CCNB1* (cyclin B1), *CCNB2* (cyclin B2) and *E2F1* (transcription factor E2F1) mRNA levels in all cells analyzed (Fig. 3B). Moreover, increased mRNA levels of *CCNA2* (cyclin A2), *CCNE1* (cyclin E1), *CCNE2* (cyclin E2) and *CDC2* (cyclin-dependent kinase 1, CDK1) were observed in all HP-treated WI-38 cells and increased mRNA levels of *CDKN2D* (p19), *TP53* (p53), *CCND3* (cyclin D3), *CDK2* (cyclin-dependent kinase 2), *CDK4* (cyclin-dependent kinase 4), *E2F4* (transcription factor E2F4) and *HDAC5* (histone deacetylase 5) were documented in all HP-treated BJ cells (Fig. 3B). HP treatment also caused a decrease in mRNA levels of *CCND1* (cyclin D1) and *CCNH* (cyclin H) in all cells analyzed (Fig. 3B). A decrease in mRNA levels of *CDK4* (cyclin-dependent kinase 4) and *CDK7* (cyclin-dependent kinase 7) was exclusively observed in HP-treated DNMT2-silenced WI-38 cells and a decrease in mRNA levels of *CCNE1* (cyclin E1) and *CCNE2* (cyclin E2) was exclusively documented in HP-treated DNMT2-silenced BJ cells (Fig. 3B). As mRNA levels of *TP53* (p53) were increased in all HP-treated BJ cells and mRNA levels of *CDKN2A* (p16) were upregulated in DNMT2-silenced BJ cells, we decided then to evaluate protein levels of p53, p16 and also p21 that is regulated by p53 (Fig. 3C and D). The levels of cell cycle inhibitors, namely p16, p21 and p53 were elevated in DNMT2-silenced cells in the control and stress conditions and the effect, except of p53, was also permanent and observed after 7 days of cell culture (Fig. 3C and D). However, upregulation of p21 (Fig. 3C and D) did not correspond to increased mRNA levels of *CDKN1A* (p21) (Fig. 3B). Perhaps, increased p21 levels are achieved by protein stabilization rather than increased *CDKN1A* gene expression. DNMT2 silencing also promoted cellular senescence as judged by increased number of senescence-associated-beta-galactosidase (SA-beta-gal) positive cells of DNMT2-silenced cells in the control conditions (Fig. 4A).

We have also considered stress-induced premature senescence (HP treatment), but DNMT2 silencing did not potentiate the action of HP in terms of the levels of SA-beta-gal positive cells (Fig. 4A). In contrast, the levels of SA-beta-gal positive cells were slightly decreased compared to HP-treated control cells (Fig. 4A). As DNMT2 silencing may stimulate cellular senescence (Fig. 4A), the protein levels of DNMT2 and DNMT2 localization were also evaluated during replicative senescence of human fibroblasts (Fig. 4B and C). Senescent cells with increased levels of p21, a biomarker of cellular senescence, were characterized by elevated levels of DNMT2 (Fig. 4B). Moreover, DNMT2 nuclear/cytosolic ratio was decreased, whereas cytosolic fraction of DNMT2 was increased in WI-38 fibroblasts during replicative senescence (Fig. 4C).

3.4. DNMT2 silencing promotes oxidative stress

The production of reactive oxygen species, ROS (total ROS, total superoxide and mitochondrial superoxide) was augmented in DNMT2-silenced fibroblasts compared to unmodified cells in the control conditions (Fig. 5A).

HP potentiated ROS production in DNMT2-depleted cells (Fig. 5A) that resulted in protein carbonylation (Fig. 5B).

3.5. DNMT2 silencing induces genomic instability

The levels of DNA damage (DNA double strand breaks) and micronuclei production were increased in DNMT2-silenced fibroblasts compared to unmodified cells in the control conditions (Fig. 6A).

DNMT2 silencing also induced DNA damage response (increased phosphorylation of ATM and H2AX) in WI-38 cells in the control conditions (Fig. 6B). HP treatment moderately intensified DNA damaging effect in DNMT2-silenced cells compared to control cells that was especially seen in WI-38 cells (Fig. 6). HP treatment promoted DNA damage response in all cell lines examined (ATM activation, H2AX phosphorylation, 53BP1 foci formation) (Fig. 6).

3.6. DNMT2 silencing results in epigenetic changes

We have then evaluated if DNMT2 silencing and HP treatment may have a prolonged effect on the expression of genes involved in DNA methylation and transcriptional repression (n = 28) after 7 days of HP removal (Fig. 7A and B).

Similar changes in the patterns of gene expression were revealed as all control samples and all HP-treated samples were grouped together (Fig. 7A). Increased mRNA levels of *DNMT3B* (DNA methyltransferase DNMT3B) were observed in all HP-treated WI-38 cells after 7 days of HP removal (Fig. 7B). As DNMT2 silencing and HP treatment may promote some permanent effects on mRNA levels of selected DNA methyltransferase genes (Fig. 7B), protein levels of DNA methyltransferase DNMT1, DNMT3A and DNMT3B were also studied (Fig. 7C and D). The levels of DNMT1 were upregulated both in the control conditions as well after HP treatment in DNMT2-silenced WI-38 and BJ cells (Fig. 7C and D). However, the levels of DNMT3A and DNMT3B were only upregulated in BJ cells (Fig. 7C and D). Surprisingly, protein levels of DNMT3B did not correspond to mRNA levels of *DNMT3B* in WI-38 cells (Fig. 7B, C and D). Moreover, DNMT2 silencing did not promote changes in global DNA methylation in the control conditions, however, HP treatment resulted in a decrease in global DNA methylation in DNMT2-silenced WI-38 and BJ cells (Fig. 7E). We have also considered the effect of DNMT2 silencing and HP treatment on *loci*-specific DNA methylation, namely the methylation of 18 S rRNA gene promoter (Supplementary Fig. 1). The methylation status of 18 S rRNA

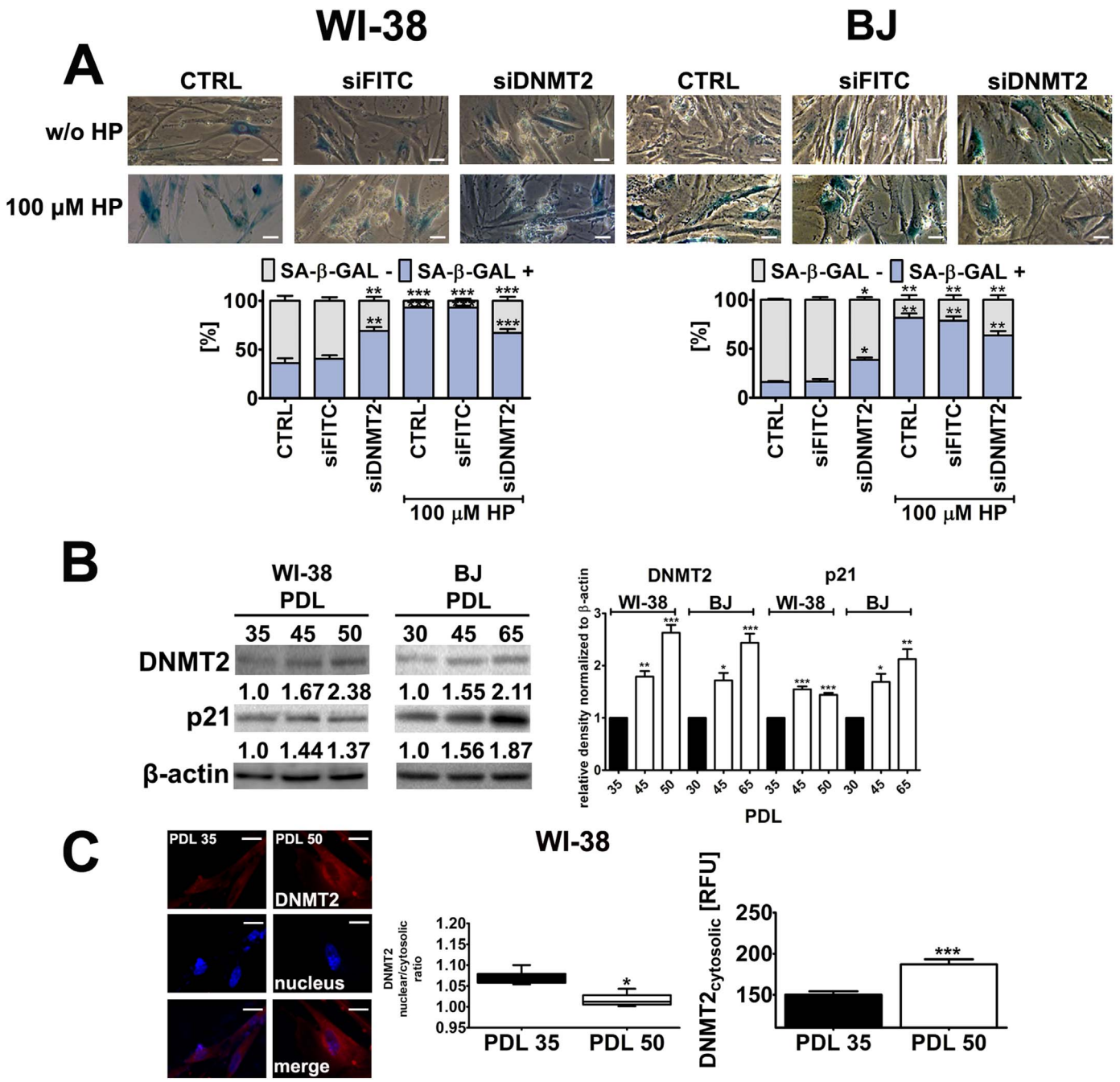

Fig. 4. DNMT2 silencing- and HP-induced premature senescence (A), upregulation of DNMT2 levels during replicative senescence in WI-38 and BJ human fibroblasts (B) and decreased DNMT2 nuclear/cytosolic ratio and increased DNMT2 cytosolic fraction during replicative senescence in WI-38 cells (C). (A) Senescence-associated β-galactosidase activity. Cells were treated with 100 μM HP for 2 h and then cultured for 7 days. Representative micrographs are shown. Scale bars 10 μm, objective 10x. Bars indicate SD, n = 3, $^{*}p < 0.05$, $^{**}p < 0.01$, $^{***}p < 0.001$ compared to CTRL (ANOVA and Dunnett's *a posteriori* test). Proliferatively active fibroblasts were used, namely WI-38 cells at PDLs from 34 to 43 and BJ cells at PDLs from 27 to 43. CTRL, non-transfected control fibroblasts; siFITC, fibroblasts transfected with control FITC-conjugated siRNA; siDNMT2, fibroblasts transfected with DNMT2 siRNA. (B) Western blot analysis of the levels of DNMT2. Data were normalized to β-actin. Replicatively senescent cells (WI-38 cells at PDL 50 and BJ cells at PDL 65) were characterized by upregulation of p21. Bars indicate SD, n = 3, $^{*}p < 0.05$, $^{**}p < 0.01$, $^{***}p < 0.001$ compared to PDL 35 (WI-38 cells) or PDL 30 (BJ cells) (ANOVA and Dunnett's *a posteriori* test). (C) DNMT2 immunosignals (red) were analyzed using imaging cytometry (left). Nuclei were visualized using Hoechst 33342 staining (blue). Representative micrographs are shown. Scale bars 10 μm, objective 10x. WI-38 cells at PDL 35 and PDL 50 were used. DNMT2 nuclear/cytosolic ratio was calculated accordingly (middle). Box and whisker plots with minimal and maximal values are shown, n = 3, $^{*}p < 0.05$ compared to PDL 35 (ANOVA and Dunnett's *a posteriori* test). DNMT2 cytosolic signals are presented as relative fluorescence units (RFU) (right). Bars indicate SD, n = 3, $^{***}p < 0.001$ compared to PDL 35 (ANOVA and Dunnett's *a posteriori* test). (For interpretation of the references to color in this figure legend, the reader is referred to the web version of this article.)

gene promoter was unaffected upon DNMT2 silencing and HP treatment (Supplementary Fig. 1). The levels of 18S rRNA transcripts were also comparable in all HP-treated WI-38 cells (Supplementary Fig. 1). Global RNA methylation and the levels of N^6-methyladenosine (m^6A) in RNA were also unaffected upon DNMT2 silencing and HP treatment (Fig. 7E). Finally, we have addressed the effect of DNMT2 silencing on the expression of 176 miRNAs that are involved in the regulation of cell proliferation, differentiation and stress responses, and some of them are also considered as tumor suppressors (Fig. 8A and B).

DNMT2 silencing resulted in similar changes in the expression patterns of proliferation-related miRNAs in WI-38 and BJ cells as these two categories of DNMT2-depleted cells were grouped together

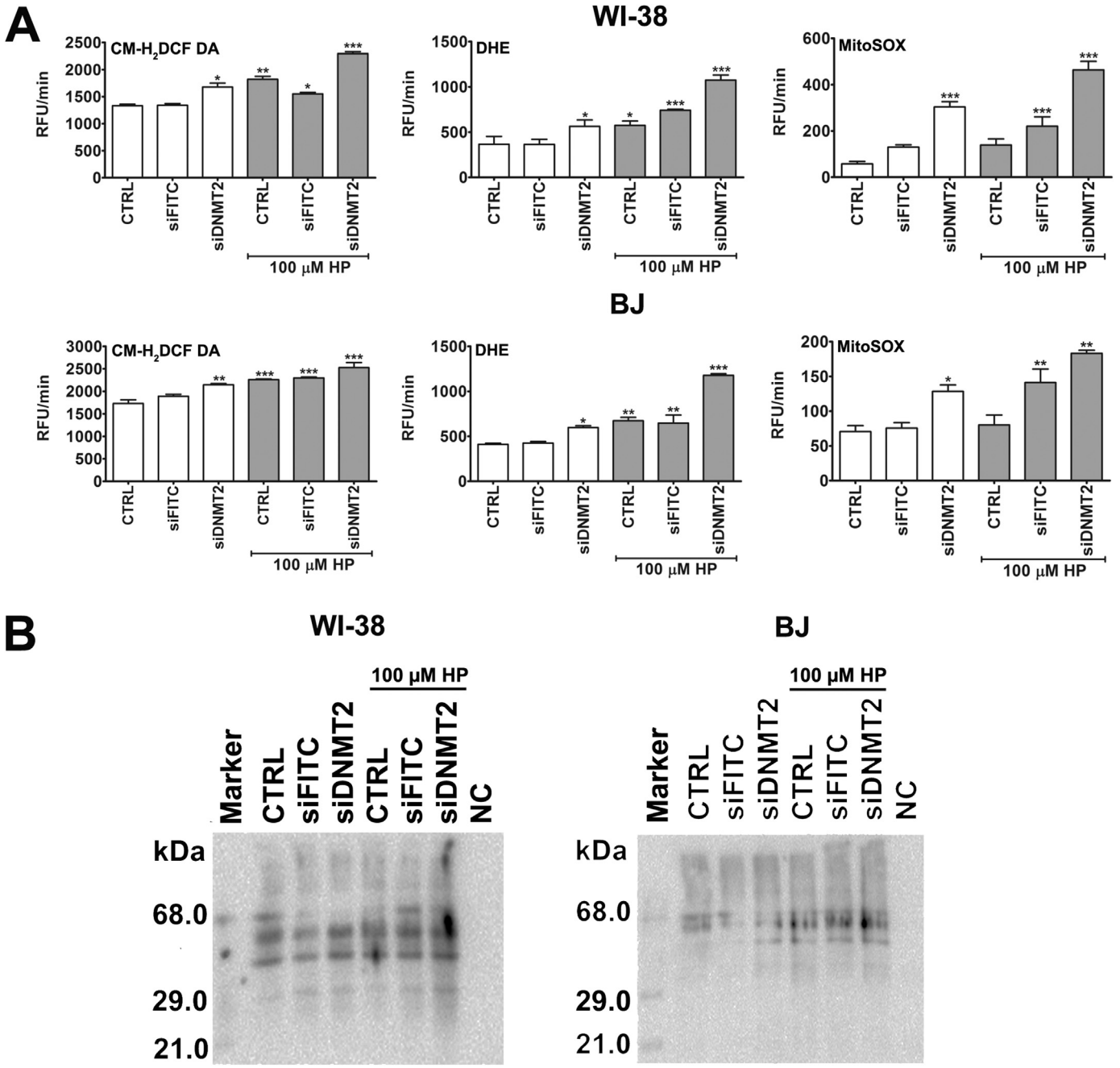

Fig. 5. DNMT2 silencing-mediated effects on reactive oxygen species production (A) and protein carbonylation (B) in WI-38 and BJ human fibroblasts. HP treatment is also considered. Cells were treated with 100 μM HP for 2 h and then cultured for 24 h. (A) Total production of reactive oxygen species (ROS), total superoxide and mitochondrial superoxide were assessed using CM-H_2DCF-DA, DHE and MitoSOX fluorogenic probes, respectively. Bars indicate SD, n = 3, $^{*}p < 0.05$, $^{**}p < 0.01$, $^{***}p < 0.001$ compared to CTRL (ANOVA and Dunnett's *a posteriori* test). (B) Protein carbonylation was revealed using OxyBlot™ Protein Oxidation Detection Kit (Merck Millipore). A negative control without DNPH derivatization (lane NC) and a positive control with a mixture of standard proteins with attached DNP residues (lane Marker) are also shown. Proliferatively active fibroblasts were used, namely WI-38 cells at PDLs from 34 to 43 and BJ cells at PDLs from 27 to 43. CTRL, non-transfected control fibroblasts; siFITC, fibroblasts transfected with control FITC-conjugated siRNA; siDNMT2, fibroblasts transfected with DNMT2 siRNA.

(Fig. 8A). We found that eleven miRNAs were significantly upregulated in DNMT2-silenced WI-38 and BJ cells, namely miR-28-3p, miR-34a-3p, miR-30b-5p, miR-29b-3p, miR-200c-3p, miR-28-5p, miR-379-5p, miR-382-5p, miR-194-5p, miR-193b-3p and miR-409-3p (Fig. 8B). The effect of control siRNA (siFITC) was also considered and control siRNA treatment resulted in upregulation of miR-181b-5p and miR-126-5p and downregulation of miR-377-3p and miR-27a-3p (Fig. 8B).

4. Discussion

We found that DNMT2-depleted WI-38 and BJ human fibroblasts are susceptible to oxidative stress and DNA damage, and DNMT2 silencing-mediated changes in the levels of proliferation-related miRNAs may shape and determine cell fate, namely may promote the inhibition of cell proliferation and cellular senescence (Fig. 8C). We propose that lowering DNMT2 levels that limits proliferative capacity may be considered as a novel anticancer strategy.

Surprisingly, control siRNA treatment resulted in upregulation of

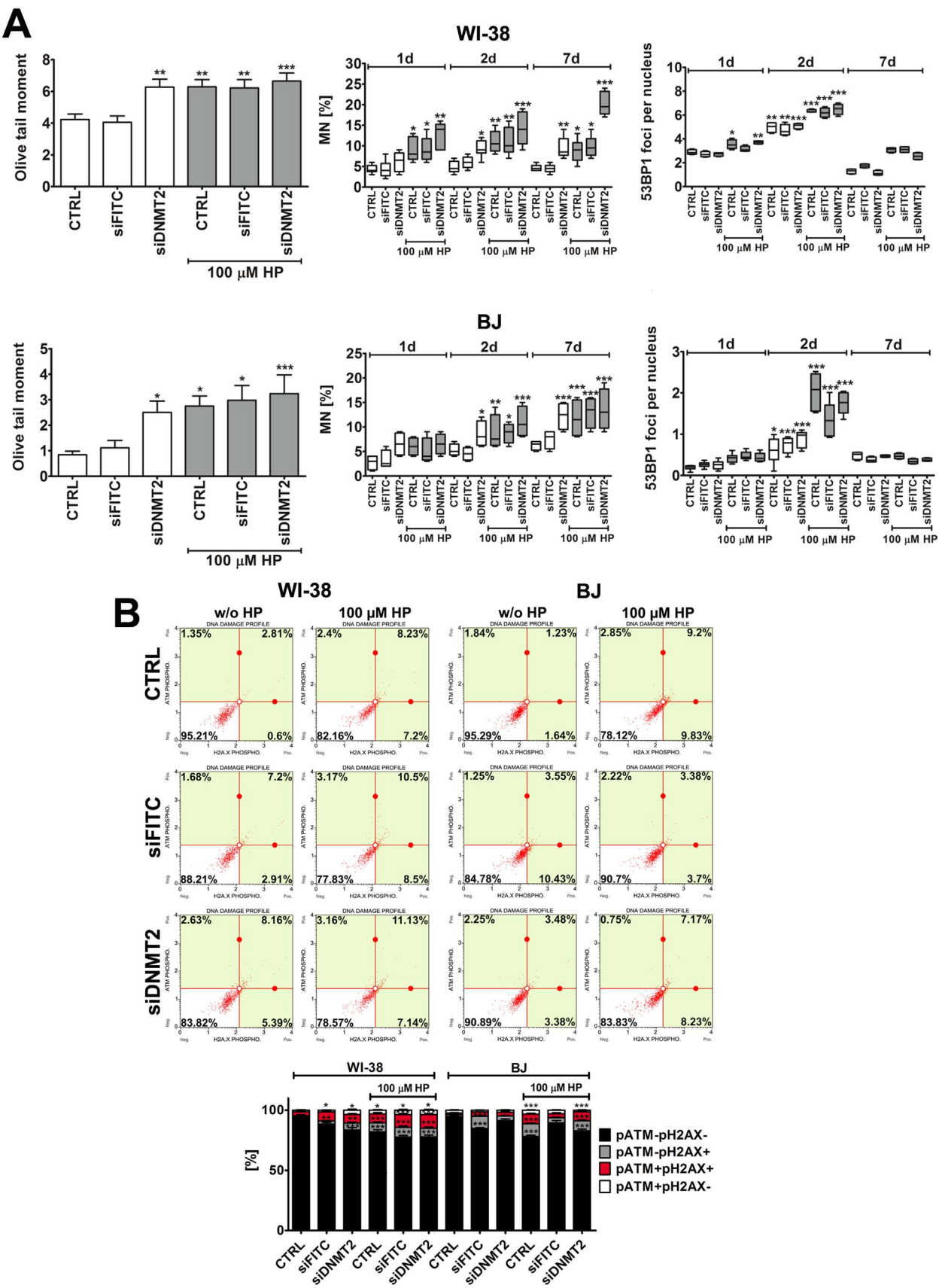

Fig. 6. DNMT2 silencing- and HP-induced genetic instability (A) and DNA damage response (DDR) (A, B) in WI-38 and BJ human fibroblasts. (A) Comet assay, micronuclei production and 53BP1 immunostaining. For comet assay, cells were treated with 100 μM HP for 2 h and then cultured for 48 h. Bars indicate SD or box and whisker plots are shown, n = 3, $^{*}p < 0.05$, $^{**}p < 0.01$, $^{***}p < 0.001$ compared to CTRL (ANOVA and Dunnett's *a posteriori* test). (B) Activation of ATM and H2AX were assessed using Muse™ Cell Analyzer and Muse™ Multi-Color DNA Damage Kit (Merck Millipore). Cells were treated with 100 μM HP for 2 h and then cultured for 48 h. Bars indicate SD, n = 3, $^{*}p < 0.05$, $^{**}p < 0.01$, $^{***}p < 0.001$ compared to CTRL (ANOVA and Dunnett's *a posteriori* test). Proliferatively active fibroblasts were used, namely WI-38 cells at PDLs from 34 to 43 and BJ cells at PDLs from 27 to 43. CTRL, non-transfected control fibroblasts; siFITC, fibroblasts transfected with control FITC-conjugated siRNA; siDNMT2, fibroblasts transfected with DNMT2 siRNA.

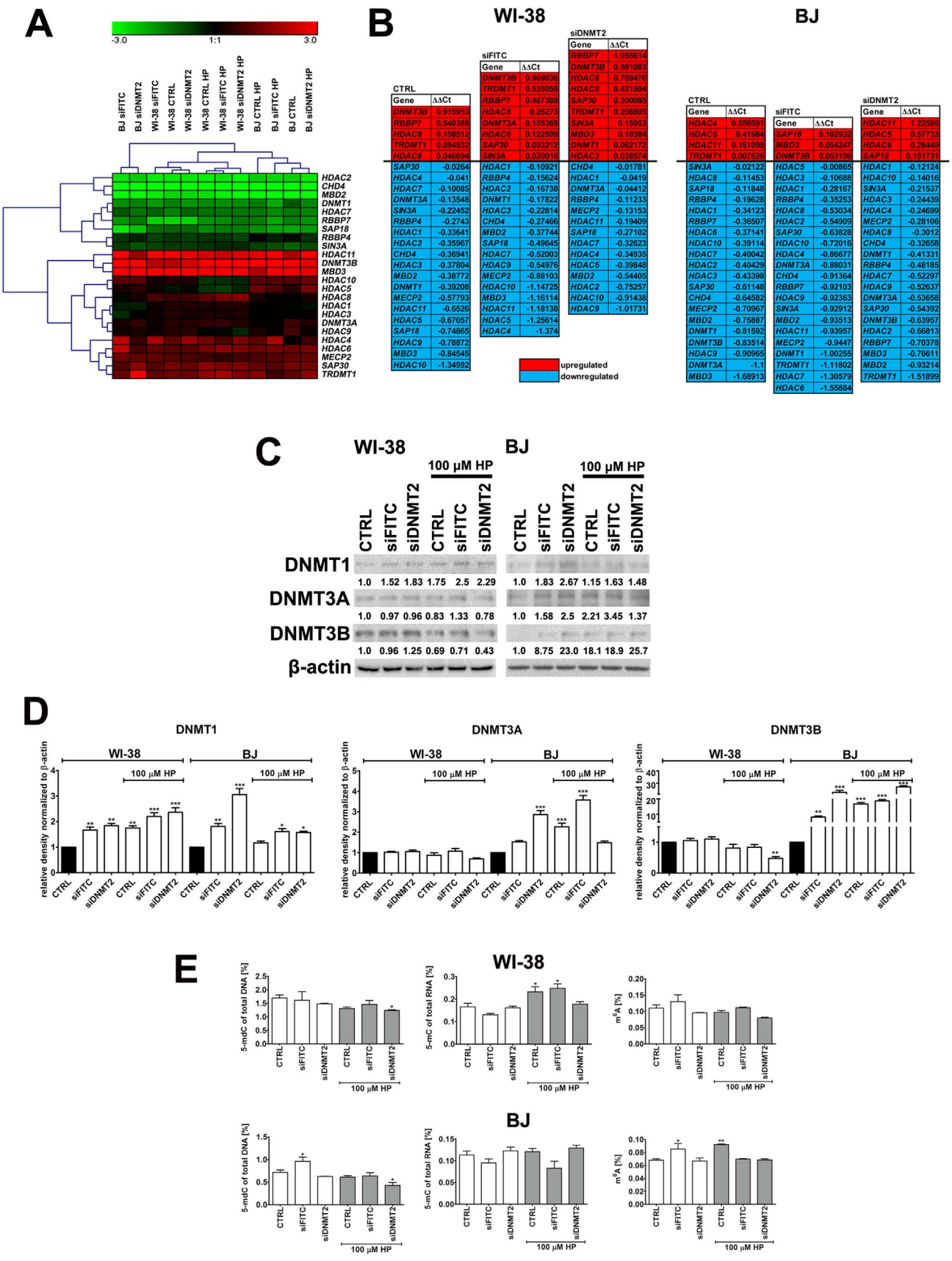

(caption on next page)

Fig. 7. DNMT2 silencing- and HP-mediated changes in DNA and RNA methylation parameters in WI-38 and BJ human fibroblasts. (A, B) The expression of selected genes involved in DNA methylation and transcriptional repression. Cells were treated with 100 μM HP for 2 h and then cultured for 7 days. (A) A heat map generated from qRT-PCR data is shown. Hierarchical clustering was created using Genesis 1.7.7 software. (B) HP-mediated up- (red) and downregulation (blue) of DNA methylation and transcriptional repression genes. ΔΔCt values are shown. (C, D) Western blot analysis of the levels of DNMT1, DNMT3A and DNMT3B. Cells were treated with 100 μM HP for 2 h and then cultured for 24 h. Data were normalized to β-actin. (D) Bars indicate SD, n = 3, $^{*}p < 0.05$, $^{**}p < 0.01$, $^{***}p < 0.001$ compared to CTRL (ANOVA and Dunnett's *a posteriori* test). (E) The levels of 5-methyldeoxycytosine (5-mdC) in DNA samples and the levels of 5-methylcytosine (5-mC) and N^6-methyladenosine (m^6A) in RNA samples were measured using MethylFlash™ Methylated DNA 5-mdC Quantification Kit, MethylFlash 5-mC RNA Methylation ELISA Easy Kit and EpiQuik m^6A RNA Methylation Quantification Kit (EpiGentek), respectively. Cells were treated with 100 μM HP for 2 h and then cultured for 7 days (DNA methylation) and 24 h (RNA methylation). Bars indicate SD, n = 3, $^{*}p < 0.05$, $^{**}p < 0.01$ compared to CTRL (ANOVA and Dunnett's *a posteriori* test). Proliferatively active fibroblasts were used, namely WI-38 cells at PDLs from 34 to 43 and BJ cells at PDLs from 27 to 43. CTRL, non-transfected control fibroblasts; siFITC, fibroblasts transfected with control FITC-conjugated siRNA; siDNMT2, fibroblasts transfected with DNMT2 siRNA. (For interpretation of the references to color in this figure legend, the reader is referred to the web version of this article.)

DNMT2 mRNA levels (this study) that may suggest that DNMT2 may play a role in antiviral response in human fibroblasts. This may also account for partial but not complete silencing of *DNMT2* gene (mRNA levels) upon DNMT2 siRNA stimulation. At DNMT2 protein levels, DNMT2 silencing was the most accented during oxidative stress conditions (HP treatment) in both cell lines used. Perhaps, remaining DNMT2 protein pools are not adequately degraded in control conditions compared to stress conditions. Thus, control and stress conditions were considered in further analyses.

In general, siRNA treatment, both control siRNA and DNMT2 siRNA, promoted an increase in the levels of beta-interferon in WI-38 and BJ cells (this study). More recently, the role of DNMT2 homologs during viral infections has been proposed in different biological model systems [31–33]. In *Drosophila melanogaster*, dDnmt2 has been reported to be required for innate immune responses and *dDnmt2* mutant flies accumulated increasing levels of *Drosophila* C virus (DCV) and showed activated innate immune responses [31]. Moreover, in mosquitoes (*Aedes aegypti*), the introduced endosymbiont, *Wolbachia*, suppressed expression of *AaDnmt2*, but dengue virus (DENV) induced expression of *AaDnmt2* and the authors concluded that AaDnmt2 plays an important role not only in the maintenance of *Wolbachia* infection in mosquito cells, but also in the resistance of mosquito cells to DENV infection [32]. Finally, it has been reported that cytosine methylation by DNMT2 promoted stability and survival of HIV-1 RNA in the host cell during infection [33]. As siRNA treatment resulted in elevated levels of beta-interferon in WI-38 and BJ cells (this study) and prolonged beta-interferon stimulation induced ROS-mediated DNA damage signaling and p53-dependent senescence in IMR90 human fibroblasts [34], we decided then to analyze the effects of DNMT2 silencing on cell proliferation and longevity, intracellular redox equilibrium, genetic stability and epigenetic parameters. Lowering DNMT2 levels limited proliferative capacity and induced cellular senescence in WI-38 and BJ fibroblasts that was accompanied by elevated levels of cell cycle inhibitors p16, p21 and p53, oxidative stress, DNA damage and changes in the levels of miRNAs involved in the regulation of cell proliferation (this study). More recently, it has been shown that a sustained treatment with beta-interferon triggered a p53-dependent senescence program in IMR90 human fibroblasts [34]. Beta-interferon induced a DNA signaling pathway, the phosphorylation of p53 at serine 15 and its transcriptional activity, and beta-interferon-treated fibroblasts accumulated gamma-H2AX foci and phosphorylated forms of ATM and CHK2 [34]. DNA damage response (DDR) was activated by an increase in reactive oxygen species (ROS) induced by beta-interferon and was inhibited by the antioxidant *N*-acetyl cysteine [34]. Moreover, senescent cells with persistent DDR signaling may secrete growth factors, proteases, cytokines, and other factors that have potent autocrine and paracrine activities (so called a senescence-associated secretory phenotype, SASP) [35–38] that may induce low-level, chronic, “sterile” inflammation that may initiate or promote most, if not all, major age-related diseases [39–41].

Moreover, increased levels of DNMT2 were observed in replicatively senescent WI-38 and BJ cells. DNMT2 nuclear/cytosolic ratio is also decreased during replicative senescence that is accompanied by elevated levels of cytosolic fraction of DNMT2. Our data are in agreement with previous observation that DNMT2 may relocalize from the nucleus to the cytoplasm during stress conditions [14].

To the best of our knowledge, this is the first report on DNMT2-mediated effects on cell proliferation and longevity in human cells. More recently, we have documented that CRISPR-based Dnmt2 silencing in NIH3T3 mouse immortalized fibroblasts resulted in a decrease in telomere length and telomerase activity that caused permanent inhibition of cell proliferation and cellular senescence [22]. The role of dDnmt2 in retrotransposon silencing and telomere integrity has been also proposed in *Drosophila* and telomere protection is supposed to be achieved by dDnmt2-mediated DNA methylation [42]. Overexpression of dDnmt2 also extended *Drosophila* life span that was mediated by resistance to oxidative stress (paraquat stimulation) [18]. Moreover, overexpression of Dnmt2 (Ehmeth) in the protozoan parasite *Entamoeba histolytica* decreased sensitivity to hydrogen peroxide and *S*-nitrosoglutathione treatments [19,20]. Thus, one can conclude that DNMT2 homologs might be involved in cellular stress responses. Indeed, DNMT2 homologs are found to be upregulated during oxidant-based stress conditions in human and mouse cells, namely in HeLa cervical cancer cells upon arsenite [14] and nanodiamond [15] treatments, in human aortic smooth muscle cells upon curcumin stimulation [16] and in HT22 mouse hippocampal neuronal cells upon silver nanoparticle treatment [17]. Human DNMT2 and mouse Dnmt2 are also upregulated under DNA-damaging conditions [15,17]. Moreover, siRNA-based silencing of DNMT2 in human fibroblasts (this study) and CRISPR-based silencing of Dnmt2 in mouse NIH3T3 cells [22] resulted in increased sensitivity to HP-induced apoptotic cell death that was mediated by elevated ROS production, protein carbonylation and genomic instability. It is postulated that in *Drosophila* and *E. histolytica,* dDnmt2- and Ehmeth-mediated oxidative and nitrosative stress resistance, respectively, is mediated by elevated levels of $tRNA^{Asp}$ methylation (the methylation of C38 in the anticodon loop of $tRNA^{Asp}$) [13,20]. However, little is known about the biological role of this RNA modification. It is suggested that dDnmt2-mediated tRNA methylation may provide protection against stress-induced tRNA cleavage in *Drosophila* [13] and may also regulate the translation of proteins containing poly-Asp sequences, e.g., protein regulators of transcription and gene expression [43]. Human DNMT2 has been also found to interact with the proteins involved in RNA processing being a component of RNA processing bodies and stress granules [14]. Upregulation of human DNMT2 [15] and mouse Dnmt2 [17] also protected RNA form degradation during oxidative stress conditions. It is postulated that the role of DNMT2 in stress granules could represent a primitive cellular defense mechanism against viral infection [14] that is in agreement with our findings that control siRNA treatment promoted upregulation of *DNMT2* mRNA levels in human fibroblasts (this study).

We have then addressed the question of whether DNMT2 silencing may affect epigenetic parameters in WI-38 and BJ cells. DNMT2 silencing resulted in DNMT1 upregulation in both WI-38 and BJ cells, and DNMT3A and DNMT3B upregulation in BJ cells, but these epigenetic changes were not accompanied by changes in global or *loci*-specific DNA methylation, namely the methylation of 18S rRNA gene promoter or changes in global RNA methylation or m^6A RNA methylation. In contrast, CRISPR-based silencing of Dnmt2 in NIH3T3 mouse

A

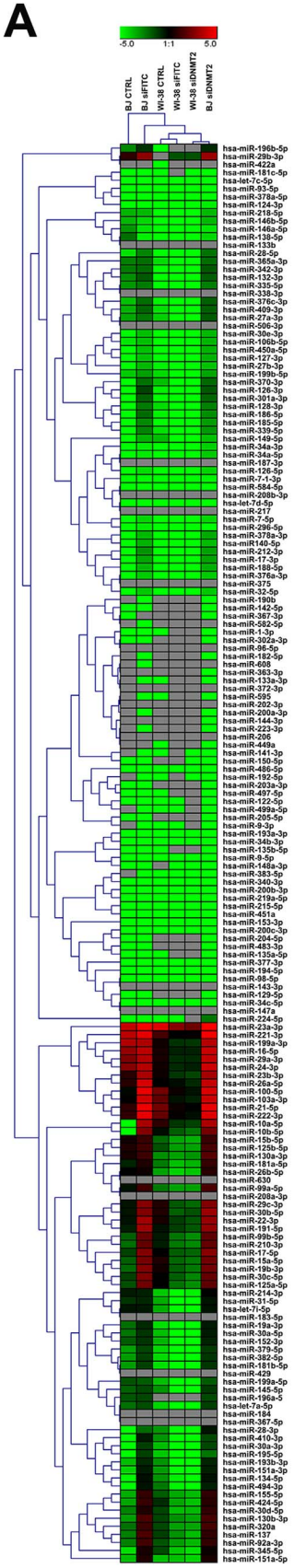

B

miR ID	fold difference [siDNMT2/siFITC]	*p* value
hsa-miR-28-3p	3.01	0.0000
hsa-miR-34a-3p	1.82	0.0478
hsa-miR-30b-5p	1.79	0.0460
hsa-miR-29b-3p	1.41	0.0185
hsa-miR-200c-3p	1.39	0.0009
hsa-miR-28-5p	1.39	0.0083
hsa-miR-379-5p	1.33	0.0221
hsa-miR-382-5p	1.25	0.0439
hsa-miR-194-5p	1.25	0.0294
hsa-miR-193b-3p	1.23	0.0381
hsa-miR-409-3p	1.18	0.0227
miR ID	**fold difference [siFITC/CTRL]**	***p* value**
hsa-miR-181b-5p	1.21	0.0240
hsa-miR-126-5p	1.12	0.0047
hsa-miR-377-3p	-1.29	0.0004
hsa-miR-27a-3p	-1.72	0.0262

upregulated
downregulated

C

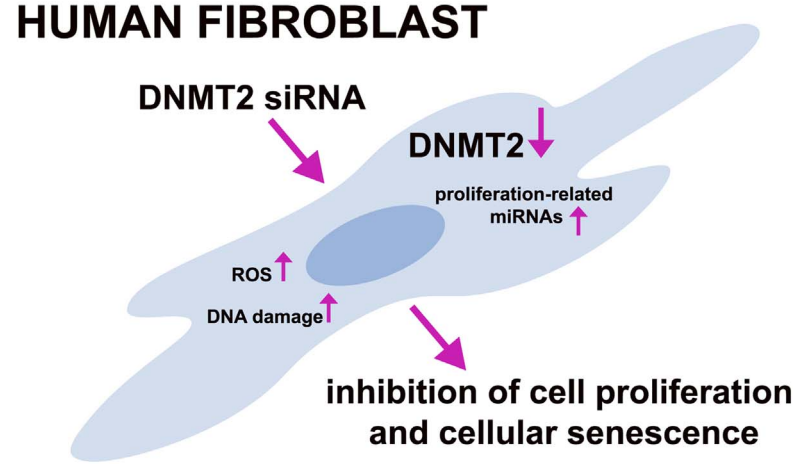

(caption on next page)

Fig. 8. DNMT2 silencing-mediated changes in miRNA profile in WI-38 and BJ human fibroblasts (A, B) and proposed miRNA-based effects on DNMT2-depleted cells (C). (A, B) The expression of 176 miRNAs was evaluated using dedicated EPIK miRNA Panel (Bioline Ltd.). (A) A heat map generated from qRT-PCR data is shown. Hierarchical clustering was created using Genesis 1.7.7 software. (B) DNMT2 silencing-mediated upregulation (red) of selected miRNAs in two fibroblast cell lines. The effect of siFITC (control siRNA) is also presented (red, upregulation; blue, downregulation). Fold difference and *p* values are shown (Student's *t*-test). Proliferatively active fibroblasts were used, namely WI-38 cells at PDLs from 34 to 43 and BJ cells at PDLs from 27 to 43. CTRL, non-transfected control fibroblasts; siFITC, fibroblasts transfected with control FITC-conjugated siRNA; siDNMT2, fibroblasts transfected with DNMT2 siRNA. (C) DNMT2 silencing in human fibroblasts promotes oxidative stress, DNA damage and changes in the levels of proliferation-related miRNAs that may result in the inhibition of cell proliferation and cellular senescence. (For interpretation of the references to color in this figure legend, the reader is referred to the web version of this article.)

fibroblasts promoted both global DNA and RNA hypermethylation, and upregulation of DNA methyltransferases, namely Dnmt1, Dnmt3a and Dnmt3b [22]. It has been postulated that DNA methyltransferases may take part in adaptive response to oxidative stress as elevated expression of DNMT1, DNMT3A and DNMT3B has been revealed in HP-treated human embryonic lung fibroblasts (HEFs) [44]. Indeed, upregulation of DNMT1 in HP-treated non-transfected WI-38 cells and upregulation of DNMT3A and DNMT3B in HP-treated non-transfected BJ cells were also observed (this study). Upregulation of DNA methyltransferases may be also considered as an adaptive response against DNA damage as a loss of Dnmt3b promoted DNA hypomethylation, chromosomal instability and spontaneous immortalization in mouse embryonic fibroblasts (MEFs) [45]. Moreover, DNA methyltransferases may also determine cell fates as human DNMT3A may induce senescence or apoptosis that depends on DNMT3A-mediated changes in the levels of p21 in doxorubicin-treated HCT116 human colorectal cancer cells [46].

Finally, DNMT2 silencing resulted in upregulation of eleven miRNAs with antiproliferative and tumor suppressive functions, namely miR-28-3p, miR-34a-3p, miR-30b-5p, miR-29b-3p, miR-200c-3p, miR-28-5p, miR-379-5p, miR-382-5p, miR-194-5p, miR-193b-3p and miR-409-3p both in WI-38 and BJ cells that may potentially affect cell proliferation in DNMT2-depleted fibroblasts. MicroRNAs (miRNAs, miRs) are a class of short, 22–25 nucleotide-long, evolutionally conserved and endogenously expressed noncoding RNA molecules that regulate gene expression in a sequence-specific manner by binding to the 3'-untranslated regions (3'-UTRs) of target mRNAs and suppressing mRNA translation and reducing mRNA stability [47–49]. Thus, miRNAs are involved in the regulation of numerous biological processes, namely development and differentiation, cell death and cell proliferation; miRNAs may also exert oncogenic (oncogenic miRNAs, oncomiRs) and tumor suppressive (tumor suppressor miRNAs, TS-miRs) effects being potentially important targets for cancer therapy [50,51]. However, one should remember that specific miRNAs can simultaneously produce competing oncogenic and tumor suppressive effects and an overall net oncogenic or net tumor-suppressive effect of miRNA may depend on the balance between miRNA-mediated upregulation or downregulation of oncogenic and tumor-suppressive pathways, the effects of the miRNA on cancer-immune system interactions and a plethora of other tumor-modifying extrinsic factors [51]. Most of upregulated miRNAs in DNMT2-silenced fibroblasts have been reported to suppress cell proliferation and promote multiple antitumor effects in different cancer models [52–62]. For example, miR-28-5p inhibited proliferation and migration by directly inhibiting RAP1B, a Ras-related small GTP-binding oncoprotein, in renal cell carcinoma [52]; miR-34a-3p reduced the proliferation of meningioma cells by targeting SMAD4, FRAT1 and BCL2 [54]; miR-30b-5p limited cell proliferation, metastasis and epithelial-to-mesenchymal transition by targeting G-protein subunit α-13 in renal cell carcinoma [55] and miR-30b-5p repressed cell proliferation by targeting DNMT3A in hepatocellular carcinoma [56]; miR-409-3p inhibited gastric cancer cell proliferation and promoted apoptosis by targeting the transcriptional regulator PHF10 [61] and miR-409-3p suppressed breast cancer cell growth and invasion by targeting Akt1 [62]. Perhaps, elevated levels of miRNAs with antiproliferative functions in DNMT2-depleted fibroblasts may also account for the inhibition of cell proliferation in WI-38 and BJ cells (this study). However, further studies are needed to reveal potential target mRNAs of these miRNAs and their role(s) in the regulation of proliferative capacity and longevity in human fibroblasts.

In summary, we have shown for the first time that DNMT2 silencing in human fibroblasts resulted in oxidative stress, genomic instability and changes in proliferation-related miRNAs that may inhibit cell proliferation and promote cellular senescence (Fig. 8C). Thus, DNMT2 may be considered as a novel regulator of cell proliferation and longevity in human fibroblasts. We speculate that the manipulation of DNMT2 levels may also exert antiproliferative effects in cancer cells and may be potentially useful anticancer approach.

Competing interests

The authors have declared that no competing interests exist.

Acknowledgments

This study was supported by Grant from Polish Ministry of Science and Higher Education, IUVENTUS PLUS 0258/IP1/2015/73. This work constitutes a part of Jagoda Adamczyk-Grochala's Ph.D. thesis. Ewa Kwasniewicz is a student of Biotechnology at University of Rzeszow, Poland.

Appendix A. Supplementary material

Supplementary data associated with this article can be found in the online version at http://dx.doi.org/10.1016/j.redox.2017.08.012.

References

[1] M. Schaefer, F. Lyko, Solving the Dnmt2 enigma, Chromosoma 119 (2010) 35–40.
[2] A. Jeltsch, A. Ehrenhofer-Murray, T.P. Jurkowski, F. Lyko, G. Reuter, S. Ankri, W. Nellen, M. Schaefer, M. Helm, Mechanism and biological role of Dnmt2 in nucleic acid methylation, RNA Biol. (2016) 1–16.
[3] A. Hermann, S. Schmitt, A. Jeltsch, The human Dnmt2 has residual DNA-(cytosine-C5) methyltransferase activity, J. Biol. Chem. 278 (2003) 31717–31721.
[4] M.G. Goll, F. Kirpekar, K.A. Maggert, J.A. Yoder, C.L. Hsieh, X. Zhang, K.G. Golic, S.E. Jacobsen, T.H. Bestor, Methylation of tRNAAsp by the DNA methyltransferase homolog Dnmt2, Science 311 (2006) 395–398.
[5] H. Ghanbarian, N. Wagner, B. Polo, D. Baudouy, J. Kiani, J.F. Michiels, F. Cuzin, M. Rassoulzadegan, K.D. Wagner, Dnmt2/Trdmt1 as mediator of RNA polymerase II transcriptional activity in cardiac growth, PLoS One 11 (2016) e0156953.
[6] M. Katoh, T. Curk, Q. Xu, B. Zupan, A. Kuspa, G. Shaulsky, Developmentally regulated DNA methylation in *Dictyostelium discoideum*, Eukaryot. Cell 5 (2006) 18–25.
[7] J. Kiani, V. Grandjean, R. Liebers, F. Tuorto, H. Ghanbarian, F. Lyko, F. Cuzin, M. Rassoulzadegan, RNA-mediated epigenetic heredity requires the cytosine methyltransferase Dnmt2, PLoS Genet. 9 (2013) e1003498.
[8] N. Kunert, J. Marhold, J. Stanke, D. Stach, F. Lyko, A Dnmt2-like protein mediates DNA methylation in *Drosophila*, Development 130 (2003) 5083–5090.
[9] M. Okano, S. Xie, E. Li, Cloning and characterization of a family of novel mammalian DNA (cytosine-5) methyltransferases, Nat. Genet. 19 (1998) 219–220.
[10] K. Rai, S. Chidester, C.V. Zavala, E.J. Manos, S.R. James, A.R. Karpf, D.A. Jones, B.R. Cairns, Dnmt2 functions in the cytoplasm to promote liver, brain, and retina development in zebrafish, Genes Dev. 21 (2007) 261–266.
[11] F. Tuorto, F. Herbst, N. Alerasool, S. Bender, O. Popp, G. Federico, S. Reitter, R. Liebers, G. Stoecklin, H.J. Grone, G. Dittmar, H. Glimm, F. Lyko, The tRNA methyltransferase Dnmt2 is required for accurate polypeptide synthesis during haematopoiesis, EMBO J. 34 (2015) 2350–2362.
[12] C.R. Wilkinson, R. Bartlett, P. Nurse, A.P. Bird, The fission yeast gene *pmt1* + encodes a DNA methyltransferase homologue, Nucleic Acids Res. 23 (1995) 203–210.
[13] M. Schaefer, T. Pollex, K. Hanna, F. Tuorto, M. Meusburger, M. Helm, F. Lyko, RNA methylation by Dnmt2 protects transfer RNAs against stress-induced cleavage, Genes Dev. 24 (2010) 1590–1595.
[14] D. Thiagarajan, R.R. Dev, S. Khosla, The DNA methyltranferase Dnmt2 participates in RNA processing during cellular stress, Epigenetics 6 (2011) 103–113.
[15] J. Mytych, A. Lewinska, A. Bielak-Zmijewska, W. Grabowska, J. Zebrowski, M. Wnuk, Nanodiamond-mediated impairment of nucleolar activity is accompanied by oxidative stress and DNMT2 upregulation in human cervical carcinoma cells,

Chem. Biol. Interact. 220C (2014) 51–63.
[16] A. Lewinska, M. Wnuk, W. Grabowska, T. Zabek, E. Semik, E. Sikora, A. Bielak-Zmijewska, Curcumin induces oxidation-dependent cell cycle arrest mediated by SIRT7 inhibition of rDNA transcription in human aortic smooth muscle cells, Toxicol. Lett. 233 (2015) 227–238.
[17] J. Mytych, J. Zebrowski, A. Lewinska, M. Wnuk, Prolonged effects of silver nanoparticles on p53/p21 pathway-mediated proliferation, DNA damage response, and methylation parameters in HT22 hippocampal neuronal cells, Mol. Neurobiol. 54 (2017) 1285–1300.
[18] M.J. Lin, L.Y. Tang, M.N. Reddy, C.K. Shen, DNA methyltransferase gene dDnmt2 and longevity of *Drosophila*, J. Biol. Chem. 280 (2005) 861–864.
[19] O. Fisher, R. Siman-Tov, S. Ankri, Pleiotropic phenotype in *Entamoeba histolytica* overexpressing DNA methyltransferase (Ehmeth), Mol. Biochem. Parasitol. 147 (2006) 48–54.
[20] R. Hertz, A. Tovy, M. Kirschenbaum, M. Geffen, T. Nozaki, N. Adir, S. Ankri, The *Entamoeba histolytica* Dnmt2 homolog (Ehmeth) confers resistance to nitrosative stress, Eukaryot. Cell 13 (2014) 494–503.
[21] A. Lewinska, P. Jarosz, J. Czech, I. Rzeszutek, A. Bielak-Zmijewska, W. Grabowska, M. Wnuk, Capsaicin-induced genotoxic stress does not promote apoptosis in A549 human lung and DU145 prostate cancer cells, Mutat. Res. Genet. Toxicol. Environ. Mutagen 779 (2015) 23–34.
[22] A. Lewinska, J. Adamczyk-Grochala, E. Kwasniewicz, M. Wnuk, Downregulation of methyltransferase Dnmt2 results in condition-dependent telomere shortening and senescence or apoptosis in mouse fibroblasts, J. Cell Physiol. (2017), http://dx.doi.org/10.1002/jcp.25848.
[23] A. Lewinska, J. Adamczyk-Grochala, E. Kwasniewicz, A. Deregowska, M. Wnuk, Diosmin-induced senescence, apoptosis and autophagy in breast cancer cells of different p53 status and ERK activity, Toxicol. Lett. 265 (2017) 117–130.
[24] N. Dworak, M. Wnuk, J. Zebrowski, G. Bartosz, A. Lewinska, Genotoxic and mutagenic activity of diamond nanoparticles in human peripheral lymphocytes *in vitro*, Carbon 68 (2014) 763–776.
[25] B.M. Gyori, G. Venkatachalam, P.S. Thiagarajan, D. Hsu, M.V. Clement, OpenComet: an automated tool for comet assay image analysis, Redox Biol. 2 (2014) 457–465.
[26] P.L. Olive, R.E. Durand, J.P. Banath, P.J. Johnston, Analysis of DNA damage in individual cells, Methods Cell Biol. 64 (2001) 235–249.
[27] A. Sturn, J. Quackenbush, Z. Trajanoski, Genesis: cluster analysis of microarray data, Bioinformatics 18 (2002) 207–208.
[28] A. Lewinska, J. Adamczyk-Grochala, E. Kwasniewicz, A. Deregowska, M. Wnuk, Ursolic acid-mediated changes in glycolytic pathway promote cytotoxic autophagy and apoptosis in phenotypically different breast cancer cells, Apoptosis 22 (2017) 800–815.
[29] K. Ghoshal, S. Majumder, J. Datta, T. Motiwala, S. Bai, S.M. Sharma, W. Frankel, S.T. Jacob, Role of human ribosomal RNA (rRNA) promoter methylation and of methyl-CpG-binding protein MBD2 in the suppression of rRNA gene expression, J. Biol. Chem. 279 (2004) 6783–6793.
[30] C. Rohde, Y. Zhang, R. Reinhardt, A. Jeltsch, BISMA–fast and accurate bisulfite sequencing data analysis of individual clones from unique and repetitive sequences, BMC Bioinform. 11 (2010) 230.
[31] Z. Durdevic, K. Hanna, B. Gold, T. Pollex, S. Cherry, F. Lyko, M. Schaefer, Efficient RNA virus control in *Dirosophila* requires the RNA methyltransferase Dnmt2, EMBO Rep. 14 (2013) 269–275.
[32] G. Zhang, M. Hussain, S.L. O'Neill, S. Asgari, *Wolbachia* uses a host microRNA to regulate transcripts of a methyltransferase, contributing to dengue virus inhibition in *Aedes aegypti*, Proc. Natl. Acad. Sci. USA 110 (2013) 10276–10281.
[33] R.R. Dev, R. Ganji, S.P. Singh, S. Mahalingam, S. Banerjee, S. Khosla, Cytosine methylation by DNMT2 facilitates stability and survival of HIV-1 RNA in the host cell during infection, Biochem. J. 474 (2017) 2009–2026.
[34] O. Moiseeva, F.A. Mallette, U.K. Mukhopadhyay, A. Moores, G. Ferbeyre, DNA damage signaling and p53-dependent senescence after prolonged beta-interferon stimulation, Mol. Biol. Cell 17 (2006) 1583–1592.
[35] J.C. Acosta, A. O'Loghlen, A. Banito, M.V. Guijarro, A. Augert, S. Raguz, M. Fumagalli, M. Da Costa, C. Brown, N. Popov, Y. Takatsu, J. Melamed, F. d'Adda di Fagagna, D. Bernard, E. Hernando, J. Gil, Chemokine signaling via the CXCR2 receptor reinforces senescence, Cell 133 (2008) 1006–1018.
[36] J.P. Coppe, C.K. Patil, F. Rodier, Y. Sun, D.P. Munoz, J. Goldstein, P.S. Nelson, P.Y. Desprez, J. Campisi, Senescence-associated secretory phenotypes reveal cell-nonautonomous functions of oncogenic RAS and the p53 tumor suppressor, PLoS Biol. 6 (2008) 2853–2868.
[37] J.P. Coppe, C.K. Patil, F. Rodier, A. Krtolica, C.M. Beausejour, S. Parrinello, J.G. Hodgson, K. Chin, P.Y. Desprez, J. Campisi, A human-like senescence-associated secretory phenotype is conserved in mouse cells dependent on physiological oxygen, PLoS One 5 (2010) e9188.
[38] T. Kuilman, C. Michaloglou, L.C. Vredeveld, S. Douma, R. van Doorn, C.J. Desmet, L.A. Aarden, W.J. Mooi, D.S. Peeper, Oncogene-induced senescence relayed by an interleukin-dependent inflammatory network, Cell 133 (2008) 1019–1031.
[39] A. Freund, A.V. Orjalo, P.Y. Desprez, J. Campisi, Inflammatory networks during cellular senescence: causes and consequences, Trends Mol. Med. 16 (2010) 238–246.
[40] H.Y. Chung, M. Cesari, S. Anton, E. Marzetti, S. Giovannini, A.Y. Seo, C. Carter, B.P. Yu, C. Leeuwenburgh, Molecular inflammation: underpinnings of aging and age-related diseases, Ageing Res. Rev. 8 (2009) 18–30.
[41] F. Rodier, J. Campisi, Four faces of cellular senescence, J. Cell Biol. 192 (2011) 547–556.
[42] S. Phalke, O. Nickel, D. Walluscheck, F. Hortig, M.C. Onorati, G. Reuter, Retrotransposon silencing and telomere integrity in somatic cells of *Drosophila* depends on the cytosine-5 methyltransferase DNMT2, Nat. Genet. 41 (2009) 696–702.
[43] R. Shanmugam, J. Fierer, S. Kaiser, M. Helm, T.P. Jurkowski, A. Jeltsch, Cytosine methylation of tRNA-Asp by DNMT2 has a role in translation of proteins containing poly-Asp sequences, Cell Discov. 1 (2015) 15010.
[44] W. Zhang, W. Ji, J. Yang, L. Yang, W. Chen, Z. Zhuang, Comparison of global DNA methylation profiles in replicative versus premature senescence, Life Sci. 83 (2008) 475–480.
[45] J.E. Dodge, M. Okano, F. Dick, N. Tsujimoto, T. Chen, S. Wang, Y. Ueda, N. Dyson, E. Li, Inactivation of Dnmt3b in mouse embryonic fibroblasts results in DNA hypomethylation, chromosomal instability, and spontaneous immortalization, J. Biol. Chem. 280 (2005) 17986–17991.
[46] Y. Zhang, Y. Gao, G. Zhang, S. Huang, Z. Dong, C. Kong, D. Su, J. Du, S. Zhu, Q. Liang, J. Zhang, J. Lu, B. Huang, DNMT3a plays a role in switches between doxorubicin-induced senescence and apoptosis of colorectal cancer cells, Int. J. Cancer 128 (2011) 551–561.
[47] V. Ambros, The functions of animal microRNAs, Nature 431 (2004) 350–355.
[48] D.P. Bartel, MicroRNAs: genomics, biogenesis, mechanism, and function, Cell 116 (2004) 281–297.
[49] L. He, G.J. Hannon, MicroRNAs: small RNAs with a big role in gene regulation, Nat. Rev. Genet. 5 (2004) 522–531.
[50] M. Negrini, M. Ferracin, S. Sabbioni, C.M. Croce, MicroRNAs in human cancer: from research to therapy, J. Cell Sci. 120 (2007) 1833–1840.
[51] A.A. Svoronos, D.M. Engelman, F.J. Slack, OncomiR or Tumor Suppressor? The duplicity of microRNAs in cancer, Cancer Res. 76 (2016) 3666–3670.
[52] C. Wang, C. Wu, Q. Yang, M. Ding, J. Zhong, C.Y. Zhang, J. Ge, J. Wang, C. Zhang, miR-28-5p acts as a tumor suppressor in renal cell carcinoma for multiple antitumor effects by targeting RAP1B, Oncotarget 7 (2016) 73888–73902.
[53] X.J. Li, Z.J. Ren, J.H. Tang, MicroRNA-34a: a potential therapeutic target in human cancer, Cell Death Dis. 5 (2014) e1327.
[54] T.V. Werner, M. Hart, R. Nickels, Y.J. Kim, M.D. Menger, R.M. Bohle, A. Keller, N. Ludwig, E. Meese, MiR-34a-3p alters proliferation and apoptosis of meningioma cells in vitro and is directly targeting SMAD4, FRAT1 and BCL2, Aging 9 (2017) 932–954.
[55] W. Liu, H. Li, Y. Wang, X. Zhao, Y. Guo, J. Jin, R. Chi, MiR-30b-5p functions as a tumor suppressor in cell proliferation, metastasis and epithelial-to-mesenchymal transition by targeting G-protein subunit alpha-13 in renal cell carcinoma, Gene 626 (2017) 275–281.
[56] X. Qin, J. Chen, L. Wu, Z. Liu, MiR-30b-5p acts as a tumor suppressor, repressing cell proliferation and cell cycle in human hepatocellular carcinoma, Biomed. Pharmacother. 89 (2017) 742–750.
[57] H. Butz, P.M. Szabo, H.W. Khella, R. Nofech-Mozes, A. Patocs, G. Yousef, M. miRNA-target network reveals miR-124as a key miRNA contributing to clear cell renal cell carcinoma aggressive behaviour by targeting CAV1 and FLOT1, Oncotarget 6 (2015) 12543–12557.
[58] J.S. Chen, H.S. Li, J.Q. Huang, S.H. Dong, Z.J. Huang, W. Yi, G.F. Zhan, J.T. Feng, J.C. Sun, X.H. Huang, MicroRNA-379-5p inhibits tumor invasion and metastasis by targeting FAK/AKT signaling in hepatocellular carcinoma, Cancer Lett. 375 (2016) 73–83.
[59] D. Wu, X. Niu, J. Tao, P. Li, Q. Lu, A. Xu, W. Chen, Z. Wang, MicroRNA-379-5p plays a tumor-suppressive role in human bladder cancer growth and metastasis by directly targeting MDM2, Oncol. Rep. 37 (2017) 3502–3508.
[60] E. Mets, J. Van der Meulen, G. Van Peer, M. Boice, P. Mestdagh, I. Van de Walle, T. Lammens, S. Goossens, B. De Moerloose, Y. Benoit, N. Van Roy, E. Clappier, B. Poppe, J. Vandesompele, H.G. Wendel, T. Taghon, P. Rondou, J. Soulier, P. Van Vlierberghe, F. Speleman, MicroRNA-193b-3p acts as a tumor suppressor by targeting the MYB oncogene in T-cell acute lymphoblastic leukemia, Leukemia 29 (2015) 798–806.
[61] C. Li, H. Nie, M. Wang, L. Su, J. Li, B. Yu, M. Wei, J. Ju, Y. Yu, M. Yan, Q. Gu, Z. Zhu, B. Liu, MicroRNA-409-3p regulates cell proliferation and apoptosis by targeting PHF10 in gastric cancer, Cancer Lett. 320 (2012) 189–197.
[62] G. Zhang, Z. Liu, H. Xu, Q. Yang, miR-409-3p suppresses breast cancer cell growth and invasion by targeting Akt1, Biochem. Biophys. Res. Commun. 469 (2016) 189–195.